ENGINEER - Vol. LVIII, No. 03, pp. [27-35], 2025

DOI: https://doi.org/10.4038/engineer.v58i3.7703

Circulation Current Patterns Behind Submerged Breakwaters

R.S. Ranasinghe and G.N. Paranavithana

Abstract: The benefits of submerged breakwaters, compared to their fully emergent counterparts, remain under-utilized due to limited understanding of wave evolution and current generation near these structures. This knowledge gap has certainly restricted their application in coastal protection efforts. The present study aims to address this by visualizing and quantifying nearshore circulations behind solid and porous submerged breakwaters, using a particle tracking velocimetry technique in a small-scale laboratory experiment. Preliminary design guidelines are proposed based on the findings. The research specifically investigates the development of converging circulations closer to the shoreline and identifies the key influencing parameters. The results are applicable to systems with three submerged breakwaters or arrays of submerged breakwaters extending along the shore. Additionally, these findings can help validate numerical models, contributing to improved designs for submerged breakwater systems.

Keywords: Coast protection, Nearshore currents, Wave breaking, Channel flow, Wave-current interaction

1. Introduction

The rapid expansion of activities in coastal zones has made it increasingly important to emphasize the protection of coasts worldwide against erosion. Over the past few decades, this topic has gained significant attention, prompting many local authorities to adopt measures that are effective, stable, environmentally sustainable, and economically viable for mitigating shoreline erosion.

Various techniques can be employed to stabilize eroding coasts. Soft measures, such as beach nourishment and berm management, are appealing due to their non-destructive nature. However, concerns about the longevity of these soft measures often arise. As a result, coastal engineers are compelled to implement hard measures, such as offshore breakwaters, seawalls, and revetments. These hard measures, while effective, tend to compromise the aesthetic appeal of a beach. As a result, submerged breakwaters have gained attention due to their numerous advantages over other hard measures. However, the lack of established design guidelines remains a significant challenge, largely due to the complex hydrodynamic conditions and the multitude of environmental and structural parameters associated with these structures. Ranasinghe et al. [1] highlighted that achieving a comprehensive understanding of hydro-morphodynamics in the vicinity of submerged structures is practically difficult when relying solely on physical model tests and/or field studies. The variation in circulation patterns, such as 2-cell or 4-cell formations, in the lee of these structures under differing conditions adds further complexity to their design. Therefore, it is crucial to thoroughly understand the development of these circulation currents before utilizing submerged breakwaters for coastal protection. If not designed properly, submerged breakwaters can lead to erosion in their lee ([2],[3],[4]) rather than accretion. Consequently, designing submerged breakwaters solely based on wave transmission characteristics is insufficient and unsatisfactory.

Several researchers have explored the evolution of nearshore circulations behind submerged breakwaters and the resulting shoreline responses to these structures, employing physical, numerical, and analytical modelling techniques. Ranasinghe et al. [5] utilized the MIKE21 CAMS model to study the morphological evolution behind a V-shaped artificial surfing reef through both physical and numerical modelling approaches.

*Eng.(Dr). **R. S. Ranasinghe**, AMIE(SL), B.Sc. Eng. (Hons), M.Eng. (Tokyo), D. Eng. (Tokyo), Senior Lecturer, Teesside University, UK.*
Email:R.Ranasinghe@tees.ac.uk
https://orcid.org/0000-0003-1168-0577
*Eng.(Dr). **G. N. Paranavithana**, AMIE(SL), B.Sc. Eng. (Hons), M.sc. Eng., PhD(Saitama), Senior Lecturer, The Open University of Sri Lanka.*
Email:gnpar@ou.ac.lk
https://orcid.org/0000-0001-6223-613X

The study demonstrated that a 2-cell circulation pattern forms when the structure is positioned close to the shoreline, while a 4-cell circulation pattern emerges when it is placed farther away. Figure 1 illustrates a definition sketch of these 2-cell and 4-cell circulation current systems behind submerged breakwaters.

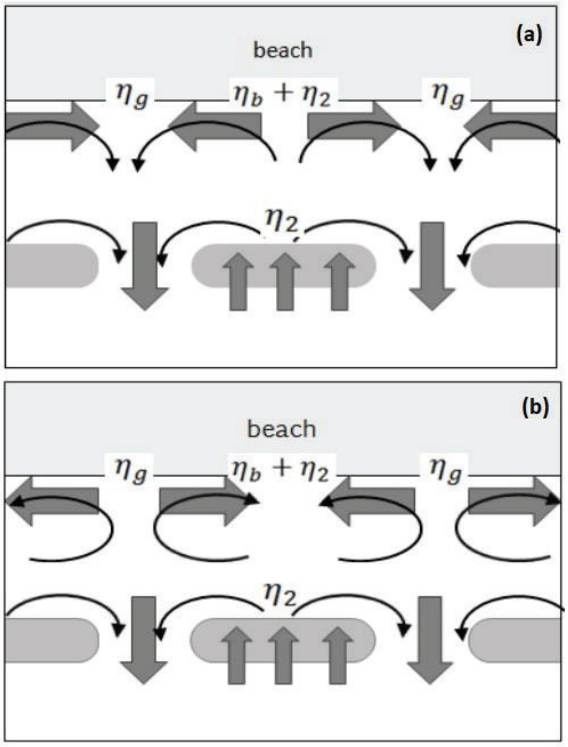

Figure 1 - 2-cell (a) and 4-cell (b) circulation Systems behind Submerged Breakwaters (Vilani et al. [6])

Ranasinghe and Sato [7] studied the morphological evolution around an impermeable submerged breakwater subjected to obliquely incident waves. They visualized circulation currents in the lee of the structure at various time intervals on a movable bed and linked the resulting accretion and erosion patterns to these flow dynamics. Following the approach of Black and Andrews [8], they concluded that a submerged breakwater should not be positioned farther than 1.77 times its alongshore length from the undisturbed shoreline to maintain positive sinuosity at the shoreline.

Ranasinghe et al. [1] conducted numerical simulations using the MIKE21 PMS module coupled with the MIKE21 HD module to calculate nearshore currents in the lee of a single submerged breakwater. They assessed the relative significance of key environmental and structural parameters through dimensional analysis. Their findings highlighted that the mode of shoreline response depends on two non-dimensional parameters, but they stressed the necessity of large-scale experimental data to validate these results due to the lack of sufficient high-quality prototype data.

Vilani et al. [6] also examined the occurrence of either erosive or accretive circulation patterns in the lee of submerged breakwaters and developed a criterion to identify the mode of shoreline response. They utilized an analytical model (Bellotti, [9]) and validated it against the non-hydrostatic model SWASH.

Previous research on circulation patterns behind submerged structures has primarily focused on the mode of shoreline response, with limited attention given to the strength and relative significance of these circulations. Ranasinghe et al. [10] conducted small-scale laboratory experiments in an 11 m × 6.5 m × 0.3 m directional wave basin at the University of Tokyo, Japan, to visualize circulation patterns behind a system of three submerged breakwaters (175 cases) and an array of submerged breakwaters (89 cases). Using solid submerged breakwater models made of concrete, they investigated the scales of these circulations and their distances from the shoreline to identify influential environmental and structural parameters. Their findings revealed that converging circulations develop when the breakwaters are positioned at a distance greater than 1.19 times their length. Additionally, they demonstrated that the gap between two submerged breakwaters should be approximately 0.35 times their length to achieve enhanced converging circulation. The study emphasized the importance of both the gap width-to-breakwater length ratio and the cross-shore distance-to-breakwater length ratio. However, no design guidelines were proposed for an array of submerged breakwaters.

The present study seeks to re-analyze the circulation patterns observed in Ranasinghe et al. [10] and expand their work to examine circulation patterns behind porous submerged breakwaters.

2. Methodology

2.1 Laboratory experimental set-up

All laboratory experiments were conducted in two facilities at the University of Tokyo, Japan: a directional wave basin measuring 11 m × 6.5 m × 0.3 m, and a wave flume measuring 35 m × 0.6 m × 1.0 m. Both facilities were equipped with wave paddles capable of absorbing reflected waves. The slopes of the wave basin and wave flume were 1:20 and 1:30, respectively. Tests were carried out under various wave conditions (with regular, normally incident waves) and structural configurations. The solid submerged structural models used in the tests by Ranasinghe et al. [10]) were constructed from concrete, while the porous models used in this study were made of gravel with a mean diameter (d_{50}) of 12 mm (see Figure 2). Both models featured a crown width of 30 cm.

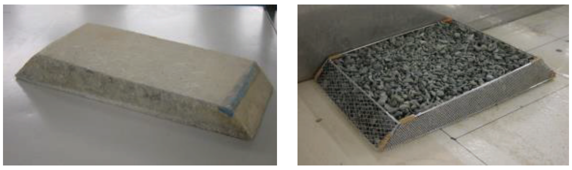

(a) Solid structures (b) Porous structures

Figure 2 - Solid structure models used in ranasinghe et al. [10] and porous structure models used in this study

The layout of the experimental set-up (plan view) is shown in Figure 3, where L_S is the length of the submerged breakwater, X is the distance to the centre of the breakwater from the still water shoreline, G is the gap between two breakwaters, and B is the crown width of the structures. In wave basin experiments, one smooth, reflective, vertical wall was used on one side to replicate the hydrodynamics around three submerged breakwaters. Ranasinghe et al. [10] used two smooth, reflective, vertical walls (which can be easily adjustable to alter the width of the test channel) at both sides to replicate the hydrodynamics around an array of breakwaters. However, no cases involving an array of porous submerged breakwaters were conducted in the wave basin for the present study; these tests were instead performed in the wave flume. During the wave flume experiments, the side vertical walls were smooth and reflective, effectively replicating the hydrodynamics around an array of structures. Figure 3(a) illustrates the arrangement for three structures in the wave basin, while Figure 3(b) shows the arrangement for an array of structures in the wave flume.

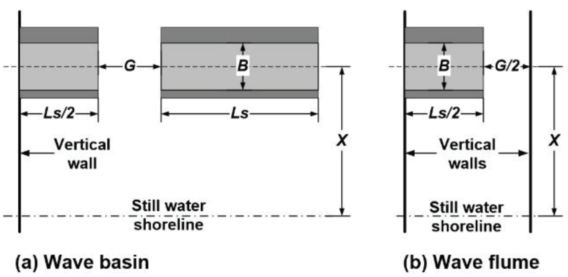

Figure 3 - Layout of the experimental set-up in the wave basin (a) and the wave flume (b)

Table 1 presents the offshore wave conditions used in this study. In the wave basin experiments, the offshore wave height was set to either 2.5 cm or 3.5 cm, while the wave period was varied between 0.8 s, 1.25 s, and 1.6 s. This resulted in a total of 60 test cases for porous structures with different configurations. Each wave condition (WB01, WB03, WB04, WB06, WB07, WB09) was applied to a three-breakwater porous system, with the freeboard (F_b) set to either 1 cm or 2 cm, and the gap width (G) set to 10 cm, 20 cm, 30 cm, 40 cm, or 60 cm. The breakwater length (L_S) and offshore distance (X) were fixed at 112 cm and 100 cm, respectively.

Table 1 - Wave conditions used for the experiments in the present study

Wave condition	Offshore wave height, H (cm)	Wave period, T (s)
WB01	3.5	1.0
WB02	3.0	1.0
WB03	2.5	1.0
WB04	3.5	1.25
WB06	2.5	1.25
WB07	3.5	1.6
WB09	2.5	1.6
WF01	3.8	0.8
WF02	3.8	1.0
WF03	3.8	1.25
WF04	3.8	1.6
WF05	3.8	1.0
WF06	5.0	1.0
WF07	7.0	1.0
WF08	5.0	0.8
WF09	5.0	1.25
WF10	5.0	1.6

The wave flume experiments included ten (10) cases forced with ten different offshore wave conditions (WF01-WF10). Table 2 presents the dimensions associated with the layouts of both wave basin and wave flume experiments.

Table 2 - Dimensions associated with the layouts of wave basin and wave flume experiments

Wave condition	F_b (cm)	G (cm)	L_S (cm)	X (cm)
WB01	1,2	10,20,30,40,60	112	100
WB03	1,2	10,20,30,40,60	112	100
WB04	1,2	10,20,30,40,60	112	100
WB06	1,2	10,20,30,40,60	112	100
WB07	1,2	10,20,30,40,60	112	100
WB09	1,2	10,20,30,40,60	112	100
WF01 – WF04	2.8	40	80	200
WF05 – WF10	1.4	40	80	170

In small-scale laboratory experiments, linear scaling ratios typically range from 1:50 to 1:100. These correspond to time scales ratios of approximately 1:7 to 1:10, based on Froude number similarity. For instance, a linear scale of 1:50 can be extrapolated to represent prototype conditions with offshore wave heights between 1.25 m and 1.75 m, and wave periods ranging from 5.6 to 11.2 seconds (based on wave basin experiments). Therefore, the scale is generally appropriate for these experiments that primarily investigate gravity-driven phenomenon. While Froude scaling is generally applied for gravity-driven wave phenomenon, the flow within a porous medium is governed by different physical properties of the porous material and is highly sensitive to Reynolds number. Although 12 mm gravel is relatively coarse for a small-scale model, this is generally appropriate for minimizing viscous effects in porous media. For submerged breakwaters, the damping mechanism is often a combination of flow resistance and turbulence generation within the porous matrix. To accurately model this, the flow within the model breakwater should ideally be in a similar flow regime (the flow within a prototype breakwater will likely be in a non-linear or turbulent regime). However, perfect similarity of porous flow characteristics is still challenging due to inherent incompatibility of Froude and Reynolds scaling.

2.2 Particle tracking velocimetry (PTV) technique

The circulation patterns were visualized using the Particle Tracking Velocimetry (PTV) technique. In this method, red-coloured plastic balls with a diameter of 6 mm and a specific gravity of 1.05 were used as tracer particles. A video clip was recorded by positioning a camera vertically above the flow field. This footage was then processed and analysed sequentially to determine the magnitude and direction of the tracer particles' movement. The velocity of each tracer particle was estimated using two successive images, with each particle's identity assumed to be the closest matching particle in the following image. By tracking the particles across successive frames, their trajectories were mapped over multiple wave cycles. Velocity vectors were then calculated by dividing the displacement vectors by the time interval between two consecutive images (Ranasinghe et al. [11]).Figures 4 and 5 show images extracted from video clips recorded during the wave basin and wave flume experiments, respectively.

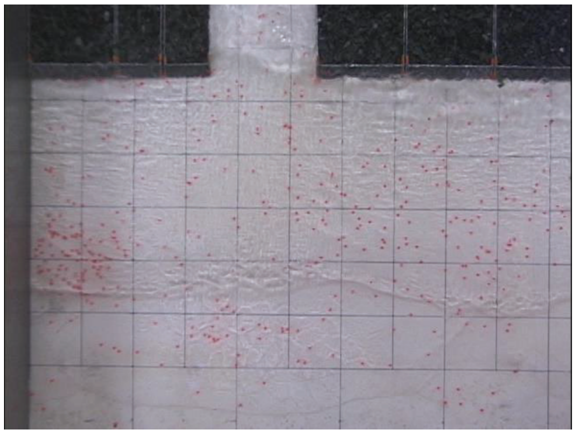

Figure 4 - An image extracted from a video clip of one of the wave basin experiments

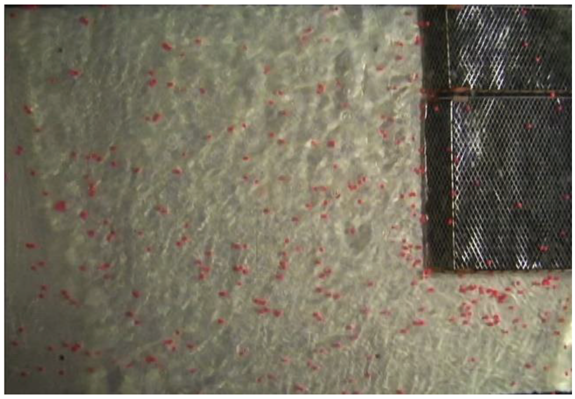

Figure 5 - An image extracted from a video clip of one of the wave flume experiments

2.3 Analysis of circulations

Assuming that a large converging circulation in the lee of a submerged breakwater, closer to the shoreline, would enhance sediment entrapment, Ranasinghe et al. [10] determined the size of the converging circulations from the streamline plot.

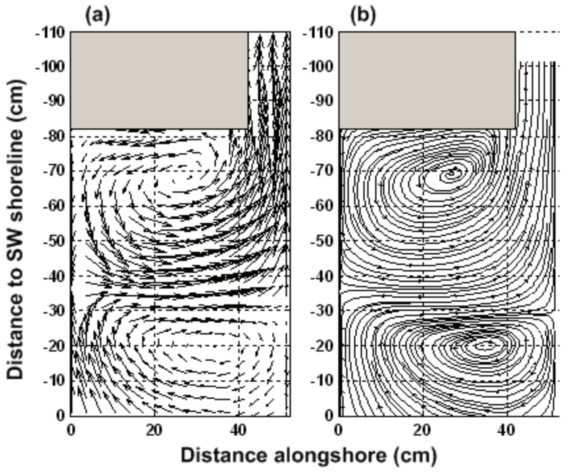

Figure 6 - The nearshore current field (a) and the corresponding streamline plot (b), ranasinghe et al. [10]

The streamline plot was created based on the current field, which was estimated using the PTV technique. Figure 6 shows the nearshore current field (a) and the corresponding streamline plot (b) from one of the experiments conducted by Ranasinghe et al. [10].

The raw experimental data of Ranasinghe et al. [10] are re-analysed in this study. As the geometry of the circulations is not exactly a circle, only three variables are introduced to define the size and the position of the circulations with minor changes to initial variables defined by them. Figure 6 depicts the new variables in the cross-shore and alongshore directions.

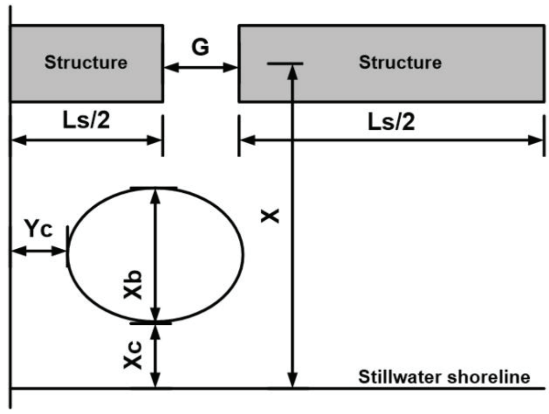

Figure 7 – Definition sketch of variables associated with the circulations

These variables are non-dimensionalized to give,

$X_c^/ = (X - X_C)/X; X_b^/ = X_b/X$

$Y_c^/ = [(L_S)/2 - Y_C)]/(L_S/2)$

$X_{C,}Y_C$ are the distance to the converging circulation from the stillwater shoreline and the centre of the breakwater system, respectively. X_b is a measure of the size of the circulation in cross-shore direction. L_S, X are the length and the offshore distance of the submerged breakwater system from the stillwater shoreline, respectively. G is the gap width between two submerged breakwaters.

The variables X_C and Y_C are generally expected to have a lower bound of zero, which results in an upper bound of unity for $X_C^/$and $Y_C^/$. This suggests that circulation occurs closer to the center of the structure and the shoreline. However, due to wave setup, X_C can sometimes take negative values under certain conditions, meaning the circulation extends beyond the stillwater shoreline. In such cases, $X_c^/$may exceed unity but will always remain positive. Conversely, $Y_C^/$ can become negative if the circulation moves further away from the structure, representing an unfavourable condition. The variable X_b, which represents the size of the circulation, is always positive. To assess the overall condition of circulation, the product of these variables is taken as:

$C = X_c^/ * Y_c^/ * X_b^/$

A high positive value of C indicates a favourable condition for converging circulations.

3. Results and Discussion

3.1 Impermeable submerged breakwater systems – ranasinghe et al. [10]

Ranasinghe et al. [10] conducted the primary set of experiments using an array of impermeable submerged breakwaters under the wave condition WB04. This wave condition was selected based on preliminary experiments that tested various wave heights and periods. The study examined three submerged breakwater systems under multiple wave conditions, including WB01, WB02, WB03, WB04, WB06, WB07, and WB09.

All the cases tested and presented by Ranasinghe et al. [10] were re-evaluated to identify converging circulation patterns. The associated non-dimensional quantities for these circulations were also calculated to obtain C. Additionally, the gap width and offshore distance of the submerged breakwaters were non-dimensionalized as follows:

Non-dimensional gap width = G/L_S
Non-dimensional offshore distance = X/L_S

Figures 8 and 9 illustrate the variation of C with G/L_S and X/L_S for an array of impermeable submerged breakwaters and a three-breakwater system, respectively. Due to minimal variations observed, the effects of freeboard and breakwater width have been disregarded in this evaluation (due to the shallow water depths used in the models; the freeboard was kept relatively constant). However, under real-world conditions, sea levels are dynamic, making the freeboard a variable parameter that fluctuates over time. The white patches in both figures indicate areas where no converging circulation occurs in the lee of the submerged breakwaters. Figure 8 reveals three possible peak conditions for optimal circulation in an array of impermeable submerged breakwaters:

- $\frac{G}{L_S} \approx 0.7$ and $\frac{X}{L_S} \approx 1.05$
- $\frac{G}{L_S} \approx 1.4$ and $\frac{X}{L_S} \approx 1.4$
- $\frac{G}{L_S} \approx 1.8$ and $\frac{X}{L_S} \approx 2.0$

Ranasinghe et al. [10] attributed the weakening of converging circulations between the first two peaks to some level of wave blocking at a specific gap width (G). While the first peak is the most prominent, its narrow range makes it slightly unstable. As a result, the second peak is considered more favourable. The third peak is as significant as the second; however, due to its large offshore distance, it may not be practical for design applications.

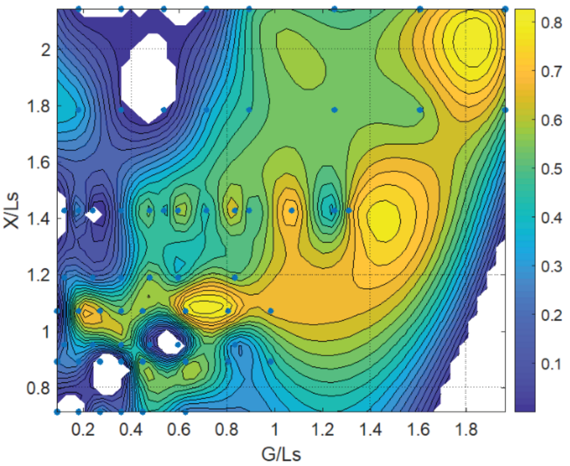

Figure 8 - Variation of parameter C with G/Ls and X/Ls for an array of impermeable submerged breakwaters

Figure 9 shows that the optimal conditions for three impermeable submerged breakwater systems occur at:

- $\frac{G}{L_S} \approx 0.4$ and $\frac{X}{L_S} \approx 1.1$
- $\frac{G}{L_S} \approx (0.6 - 1.0)$ and $\frac{X}{L_S} \approx (1.2 - 1.8)$

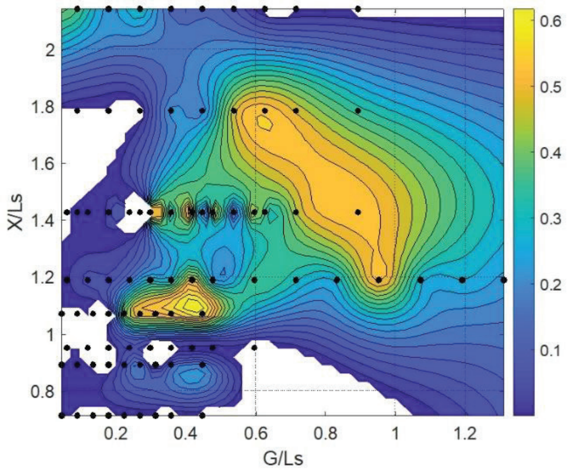

Figure 9 - Variation of parameter C with G/Ls and X/Ls for three impermeable submerged breakwater system

A similar wave-blocking phenomenon was observed in three-breakwater systems, weakening the converging circulations between the two peaks. However, the converging circulation currents behind the three-breakwater system were less pronounced than those behind the array of submerged breakwaters. This reduction in circulation strength is attributed to the easier passage of flow around the outermost breakwaters.

3.2 Porous submerged breakwater systems

As highlighted in Section 2.1, 60 cases associated with three porous submerged breakwater systems were tested in the wave basin. The porous breakwaters were expected to enhance the wave energy dissipation by porous damping. Surprisingly, none of the cases demonstrated a prominent converging circulation in the lee of three submerged breakwater systems.

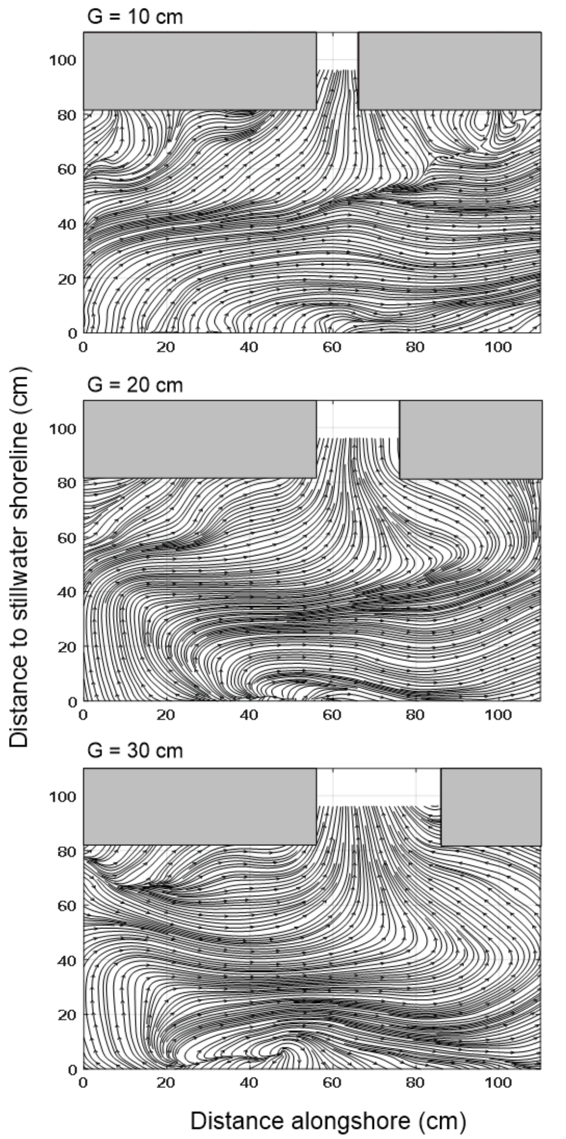

Figure 10 - Streamline plot corresponding to three porous submerged breakwater system

Unlike impermeable submerged breakwaters that dissipate the wave energy through intense wave breaking resulting in a sudden rise in the mean water level, porous breakwaters dissipate wave energy but permits water to pass through them as well. Essentially, the water flowed more evenly and smoothly around these porous breakwaters, preventing the localized water convergence typically seen behind impermeable breakwaters. Thus, the flow remained more uniform with fewer disturbances in the lee. This became more prevalent as breakwaters were placed relatively close to the shoreline which resulted only in 2-cell circulations in wave basin experiments. Figure 10 depicts the streamline plots associated with a three porous submerged breakwater system at three different gap widths, forced with wave condition WB04. This confirms the uniformity of the flow behind the three porous submerged breakwater system. Although some level of convergence is observed when the gap width is increased, it was insufficient to promote a noticeable converging circulation.

Ten cases were tested in the wave flume to further investigate the development of circulation currents behind porous submerged breakwaters. The dimensionless gap width, (G/L_s) was fixed at 0.5 and the dimensionless offshore distance of the breakwaters, (X/L_s) was set at either 2.1 or 2.5. These conditions were forced with wave conditions WF01-WF10.

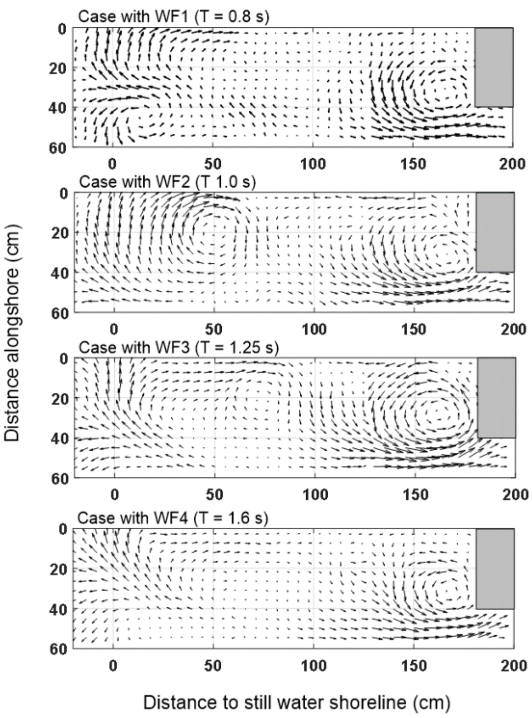

Figure 11 - Current field in the lee of an array of porous submerged breakwaters forced with an offshore wave height of 3.8 cm

Figures 11 depicts the current field in the lee of an array of porous submerged breakwaters forced with an offshore wave height of 3.8 cm but with four different wave periods. These four test cases are characterised by a dimensionless freeboard, F_b/H = 0.74 and a relatively high dimensionless offshore distance, X/L_s = 2.5. The wave condition WF02 with a wave period of 1.0 seconds is observed to generate a prominent 4-cell circulation pattern comparatively. The size of the converging circulation behind the submerged breakwater system follows a non-monotonic pattern due to the interaction between wave period and the breakwater's geometry. For small wave periods, the wavelength is small relative to the breakwater, leading to less efficient wave diffraction and weaker flow interactions behind the structure. This results in smaller circulations. As the wave period increases, the wavelength becomes larger, and the wave's energy interacts more effectively with the breakwater, amplifying the flow and generating larger circulations behind it. However, for very high wave periods, the wavelength becomes so long that the waves essentially pass over or around the breakwater without significant interaction, causing the circulation size to decrease again. Essentially, the circulation size peaks at a wave period where the breakwater efficiently resonates with the wave's energy, maximizing the induced flow.

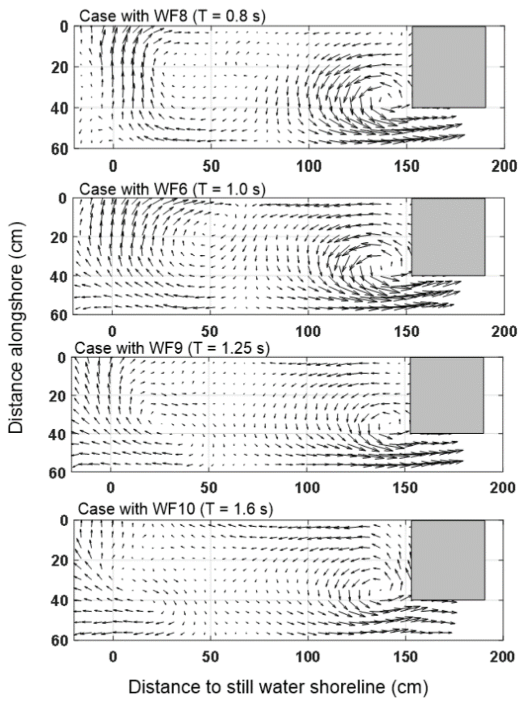

Figure 12 - Current field in the lee of an array of porous submerged breakwaters forced with an offshore wave height of 5.0 cm

Figure 12 demonstrates relatively similar circulation patterns but with stronger current velocities (which can be noticed by the magnitude of the velocity vectors through the gap). In these cases, the breakwaters have been brought closer to the shoreline and the freeboard has been made smaller. On the other hand, the offshore wave height has been increased. A larger converging circulation pattern is observed in the case associated with WF08 in comparison to WF06, WF09 and WF10, but similar to the cases in Figure 11, a prominent 4-cell converging circulation is observed in WF06 when the wave period is 1.0 second.

The weakening of circulation behind submerged breakwaters as wave height increases can primarily be attributed to the increased turbulence and complexity in wave dynamics (see Figure 13). Submerged breakwaters dissipate wave energy through reflection, refraction, and diffraction, and as the wave height increases, this dissipation becomes more pronounced. Larger waves tend to generate stronger turbulent flows and more chaotic water movement behind the breakwater. This turbulence disrupts the organized circulation patterns that are usually seen with smaller waves, resulting in a weakening or reduction in the size of the circulation.

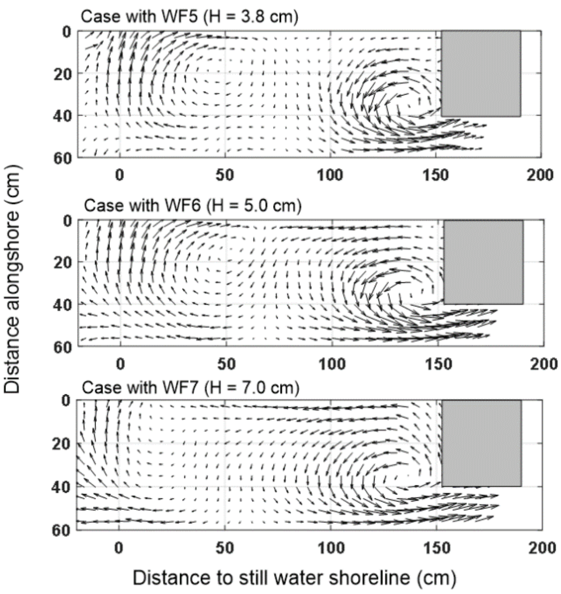

Figure 13 - Current field in the lee of an array of porous submerged breakwaters forced with a wave period of 1.0 s

Additionally, when wave height increases, the energy imparted to the water behind the breakwater increases as well. The resulting stronger currents can interact with the breakwater and induce more complex flow patterns, further disrupting the circulation. The increase in wave height also leads to increased reflection, where reflected waves may interfere with incoming waves, creating complex interference patterns that alter the flow dynamics behind the breakwater.

The combined effects of stronger turbulence, more intense currents, and complex wave interactions result in a breakdown of the previously stable circulation, causing it to weaken and shrink in size. This is why the circulation behind submerged breakwaters diminishes as wave height increases.

4. Conclusions

This study examines the circulation current patterns behind submerged breakwaters using particle tracking velocimetry in a controlled laboratory setting. The findings confirm that submerged breakwaters significantly influence nearshore hydrodynamics, leading to the formation of distinct circulation cells that impact sediment transport and shoreline morphology. Specifically, two-cell circulation patterns emerge when the breakwaters are placed closer to the shoreline, whereas four-cell patterns develop when they are positioned further offshore. These results align with previous studies and highlight the critical role of breakwater placement in determining shoreline response.

A key insight from this study is that improperly designed submerged breakwaters can induce erosion in their lee rather than promoting accretion, contradicting conventional shoreline stabilization expectations. This emphasizes the need for a more comprehensive design approach that accounts for wave transmission characteristics as well as circulation patterns. The study also demonstrates that solid and porous breakwaters generate different hydrodynamic behaviours, influencing the effectiveness of coastal protection strategies.

This study assumes that the laboratory-scale experiments accurately represent the nearshore hydrodynamics behind submerged breakwaters. The study however did not examine the strength of the circulations, which plays a critical role in influencing sediment transport and overall shoreline morphology. The study only focusses on normal incident waves and does not account for oblique wave incidence. Furthermore, porous breakwater arrays were only tested in a flume, limiting the comparative analysis. The experimental setup provides valuable insights, but limitations exist in terms of scale effects and long-term morphological evolution. Therefore, future research should incorporate large-scale physical modelling and advanced numerical simulations to further refine breakwater design guidelines.

Overall, this research enhances the understanding of circulation patterns induced by submerged breakwaters, providing a foundation for optimizing their design to achieve more effective and environmentally sustainable shoreline management. Additionally, integrating submerged breakwaters with other soft and hard engineering solutions may offer more sustainable approaches to coastal protection.

References

1. Ranasinghe, R., Larson, M. & Savioli, J., "Shoreline response to a single-parallel submerged breakwater," *Coastal Engineering*, Vol. 57 (11-12), 2010, pp. 1006–1017.

2. Deguchi, I., Sawaragi, T., "Beach fill at two coasts of different configurations",*Proceedings of the 20th International Conference on Coastal Engineering, Taipei, Taiwan,* 1986, pp. 77-86.

3. Douglass, S. L. &Weggel, J. R., "Performance of a perched beach — Slaughter beach, Delaware," *Proceedings of Coastal Sediments '87, ASCE New* York, USA, 1987, pp. 1385–1398.

4. Dean, R. G., Chen, R. & Browder, A. E., "Full scale monitoring study of a submerged breakwater Palm Beach, Florida, USA, "*Coastal Engineering*, Vol. 29, 1997, pp. 291–315.

5. Ranasinghe, R. & Turner, I., "Shoreline response to submerged breakwaters: A review," *Coastal* Engineering, Vol. 53 (1), 2006, pp. 65–79.

6. Villani, M., Bosboom, J., Zijlema, M. & Stive, M.J.F., "Circulation patterns and shoreline response induced by submerged breakwaters", *Proceedings of the 33rdInternational Conference on Coastal Engineering, Santander, Spain,* 2012, pp. 1-12.

7. Ranasinghe, R. S. & Sato, S., "Beach morphology behind single impermeable submerged breakwater under obliquely incident waves," *Coastal Engineering Journal*, Vol. 49 (1), 2007, pp. 1–24.

8. Black, K. & Andrews, C., "Sandy shoreline response to offshore obstacles: Part 1. Salient and tombolo geometry and shape, "*Journal of Coastal Research*, Special Issue 29, 2001, pp. 82–93.

9. Bellotti., G. "A simplified model of rip currents system around discontinuous submerged barriers," *Coastal Engineering Journal*, Vol. 51 (4), 2004, pp. 185–203.

10. Ranasinghe, R.S., Sato, S., Tajima, Y., Muliawan., M.J. "Evolution of nearshore currents around submerged breakwaters",*Proceedings of the 31stInternational Conference on Coastal Engineering, Hamburg, Germany,*2008, pp. 927-939.

11. Ranasinghe, R. S. & Sato, S., Tajima., Y., "Local concentration of waves due to abrupt alongshore variation of nearshore bathymetry," *Coastal Engineering Journal*, Vol. 53 (3), 2011, pp. 201–222.